

Orientation-dependent extended fine structure in electron-energy-loss spectra

M. M. Disko, O. L. Krivanek, and P. Rez*

*Department of Physics and Center for Solid State Science, Arizona State University,**Tempe, Arizona 85287*

(Received 2 November 1981)

The near-neighbor atomic environment in graphite is probed in two perpendicular directions by the selective analysis of the energy-loss spectra of 120-kV electrons scattered through such angles that the momentum exchange vector \vec{q} lies parallel and perpendicular to the graphite c axis. The radial distribution functions calculated from the extended fine structure above the carbon K edge show excellent agreement with the established atomic coordinates of graphite.

Orientation-dependent studies of the extended x-ray absorption fine structure (EXAFS) have been used as a direction-sensitive structural probe of $2H$ -WSe₂ and $1T$ -TaS₂ layered compounds,¹ single crystals of Zn,² GeS,³ ZnF,⁴ and Br adsorbed on graphite.^{5,6} The directional sensitivity is due to the fact that the ejected photoelectron wave is aligned with the polarization vector $\hat{\epsilon}_p$ of the incident x rays. In this paper we show that extended electron-energy-loss fine-structure (EXELFS) studies⁷⁻⁹ can be similarly made direction sensitive by selectively analyzing electrons that have been scattered through such angles that the corresponding momentum-transfer vector \vec{q} is aligned with a particular crystallographic direction.

Within the dipole approximation appropriate to this case,¹⁰ the EXELFS expression describing the extended fine structure due to the backscattering of the ejected photoelectron from near-neighbor atoms is identical to the EXAFS one^{6,11}:

$$k\chi(k) = \sum_i \frac{A_i(k)}{R_i^2} e^{-2k^2\sigma_i^2} e^{-2R_i/\lambda} \times \sin[2kR_i + \delta_i(k)] \cos^2\omega_i. \quad (1)$$

Here k is the magnitude of the ejected core-electron wave vector, $A_i(k)$ the backscattering amplitude from the i th atom, R_i the distance to the i th atom from the excited atom, σ_i^2 the mean-square amplitude of displacement of the i th atom from the excited atom, λ the mean-free path of the ejected electron, $\delta_i(k)$ the ejected electron wave phase shift due to both the excited atom and to the i th backscatterer, and ω_i the angle between the ra-

dial vector to the i th atom and the polarization vector $\hat{\epsilon}_p$ (for EXAFS) or the momentum-transfer vector \vec{q} (EXELFS).

The directional sensitivity arises from the term $\cos^2\omega_i$. In the x-ray case it is governed by the polarization vector of the incident radiation. In the EXELFS case it is determined¹² by the momentum-transfer vector \vec{q} , given by $\vec{q} = \vec{k}^1 - \vec{k}^0$, where \vec{k}^0 and \vec{k}^1 are the wave vectors of the fast electron before and after the collision, respectively. For a particular primary energy E_0 and energy loss E , \vec{k}^1 and hence \vec{q} are determined by the scattering angle θ [see Fig. 1(a)]. Thus different directions in a crystal may be probed simply by selecting electrons that have been scattered through different angles.^{12,13}

Graphite samples were prepared by peeling flakes from a large piece of graphite with adhesive tape. The flakes were separated from the tape in acetone, washed and centrifuged in order to remove any remaining adhesive, resuspended in acetone, and transferred onto 3-mm Cu grids covered with a holey C film. Energy-loss spectra were recorded from a 8- μ m diameter graphite region over a hole in the supporting film using a magnetic sector energy analyzer (Gatan 607) attached to a Philips EM400 electron microscope equipped with a LaB₆ gun, operating at a primary beam energy $E_0 = 120$ keV. The thickness of the graphite flake was estimated as 300 Å from a convergent beam diffraction pattern¹⁴ and also low-loss spectra.

Following Leapman and Silcox¹³ who studied the orientation dependence of the $1s \rightarrow \pi^*$ and $1s \rightarrow \sigma^*$ transitions in hexagonal boron nitride and

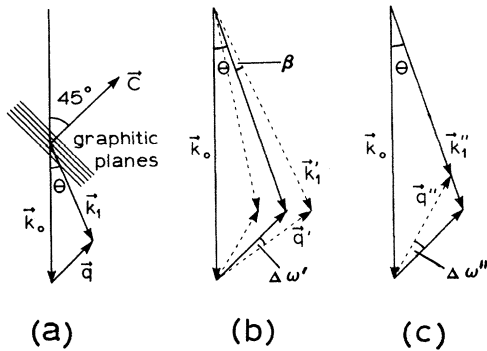


FIG. 1. Schematics illustrating the experimental geometry used for the $\vec{q}||c$ case where $\theta \approx 1.4$ mrad (a), the spread in q due to the spread in θ ($\Delta\theta = \pm\beta \approx \pm 0.6$ mrad) (b), and the variation of $|\vec{k}_1|$ with energy loss E (c).

graphite by electron-energy-loss spectroscopy, we orientated the graphite crystal with the c axis at 45° to the incident beam [Fig. 1(a)], and adjusted the beam deflection so that the spectrometer collected electrons scattered through $\theta = 1.4$ mrad (to give $\vec{q}||c$) or $\theta = -1.4$ mrad (to give $\vec{q}\perp c$). The angular spread of the incident and collected beams was determined by the finite sizes of the illumination and collection apertures (each equal to ± 0.3 mrad). Taking these factors into account, the spectrometer sampled electrons scattered into a cone with semiangle $\beta \approx 0.6$ mrad centered at $\theta = 1.4$ mrad. This relatively large angular range was necessary in order to obtain sufficiently good statistics for EXELFS analysis in a reasonable time. Thus the \cos^2 directional distribution [Eq. (1)] is broadened by $\Delta\omega'$ as shown in Fig. 1(b). A further complicating factor involves the magnitude of \vec{k}_1 , $|\vec{k}_1| \approx (1 - E/2E_0)|\vec{k}_0|$, which changes with energy loss E . This leads to a directional deviation $\Delta\omega''$ [Fig. 1(c)]. It can be compensated for by adjusting the scattering angle θ continuously as one scans through the energy loss. However, since the $\cos^2\omega_i$ distribution is a broad one, we have not performed this adjustment, preferring instead to optimize the scattering geometry so that $\vec{q}\perp c$ or $\vec{q}||c$ at 50 eV above the carbon K -edge threshold in order to simply maximize the $\vec{q}\perp c$ or $\vec{q}||c$ signal in each case. The combined effects of the finite-aperture size and variation of \vec{k}_1 with E produce a total directional deviation $\Delta\omega$ of approximately $\pm 15^\circ$ for $E = 330$ eV, and -5° , $+25^\circ$ for $E = 500$ eV ($k \approx 7 \text{ \AA}^{-1}$).

Figure 2(a) shows the graphite carbon K -edge energy-loss spectra for the two geometries acquired sequentially into 500 channels for 0.6 sec/channel. The K -edge signal has been isolated by fitting a function of the form AE^{-r} to the raw data between 180 and 280 eV, and then subtracting the extrapolated background from the edge region.¹⁵ We note that the π^* and σ^* final-state peaks exhibit the directional dependence described previously,¹⁴ but that in our case a small π^* peak remains when $\vec{q}\perp c$ due to the finite spread of \vec{q} .

The procedure used for EXELFS analysis of the carbon spectra was similar to that developed for EXAFS Fourier analysis.^{16,17} Figure 2(b) shows the extended fine structure $k\chi(k)$ extracted from each spectrum in Fig. 2(a). In both cases $k\chi(k)$ was obtained by mapping the raw energy-loss spectrum $\Psi(E)$ onto a k grid after selection of the energy loss E_i that corresponds to the ejected core-electron wave number $k=0$, i.e., $k = [2m(E - E_i)]^{1/2}$, the smooth background was removed by fitting a fifth-degree polynomial $P(k)$ to $\Psi(k)$, and finally normalizing with the smooth background $\chi(k) = [\Psi(k) - P(k)]/P(k)$. Prior to Fourier analysis of $\chi(k)$, the actual \vec{k} -space interval analyzed was selected using a square window convoluted with a narrow Gaussian.¹⁸ A lower k limit must be set in order to avoid sampling the near-edge region where valence transition and plasmon scattering effects predominate. An upper k limit is necessary because of the increasing noise

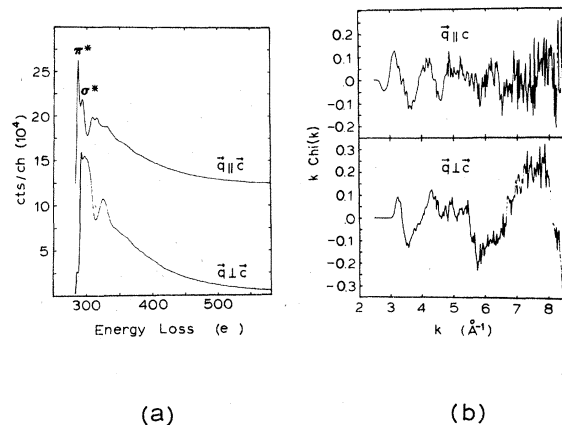


FIG. 2. Background-stripped carbon K -edges for $\vec{q}\perp c$ and $\vec{q}||c$ in graphite (a), and the extended electron energy-loss fine structure $k\chi(k)$ isolated from the graphite spectra (b). The nonoscillatory background was removed using a polynomial fit between 2.78 and 10.14 \AA^{-1} for $q||c$, and between 3.22 and 9.39 \AA^{-1} for $q\perp c$.

content at large energies above the edge. Phase-shift effects were reduced by introducing a factor $e^{-i\delta(k)}$, where $\delta(k) = \delta_{ab}(k) + \delta_{bs}(k)$, $\delta_{ab}(k)$ is the phase shift due to the ionized atom, and $\delta_{bs}(k)$ the phase shift experienced when the ejected electron wave is backscattered from a neighboring atom.¹⁶ Theoretical values for $\delta(k)$ tabulated by Teo and Lee were used for this analysis.¹⁹ The Fourier transform actually taken to obtain the EXELFS "radial distribution function" (RDF) was:

$$F(R) = \int_{k_{\min}}^{k_{\max}} \frac{k\chi(k)}{A(k)} e^{-i\vartheta(k)} e^{2ikR} dk, \quad (2)$$

where the factor k is introduced in order to cancel a $1/k$ factor in the EXELFS formula. No attempt has been made to remove amplitude effects due to $A(k)$ in Eq. (2).

The $k=0$ energy loss E_t was chosen in each case by requiring that $|F(R)|$ and $\text{Im}[F(R)]$ peak at the same radial distance R .¹⁶ The actual procedure used involved varying E_t and selecting that value where the strongest peaks in $|F(R)|$ and $\text{Im}[F(R)]$ coincide. This method yielded $E_t = 292$ eV for the $\vec{q} \perp c$ case, and 294 eV for $\vec{q} \parallel c$, or just past the σ^* peak in each case.

A carbon atom in graphite has 3 nearest neighbors at $R_1 = 1.42$ Å, 6 atoms at $R_2 = 2.42$ Å, and 3 at $R_3 = 2.85$ Å within the same (002) plane, while between the planes there are 0 or 2 neighbors at $R'_1 = C/2 = 3.35$ Å, 12 or 6 at $R'_2 = 3.64$ Å, 0 or 12 at $R'_3 = 4.13$ Å, and 12 or 6 at 4.40 Å. Thus the function $|F(R)|$ is expected to peak at 1.42 Å for $\vec{q} \perp c$, and at 3.64 Å for $\vec{q} \parallel c$. The functions $|F(R)|$ obtained from the $k\chi(k)$ data in Fig. 2(b) are shown in Fig. 3, and agree quite well with the expected result. Both R_1 for $\vec{q} \perp c$ and R'_2 for $\vec{q} \parallel c$ were accurate to within the real-space sampling interval of 0.14 Å. Peaks at $R < 3$ Å for $\vec{q} \parallel c$ are sensitive to the choice of k_{\min} and k_{\max} in Eq. (2), but there is no reasonable choice of k_{\min} and k_{\max} that causes the peak near 1.4 Å to dominate that near 3.7 Å. The substantial $|F(R)|$ values near 1.4 Å for $\vec{q} \parallel c$ and 3.7 Å for $\vec{q} \perp c$ reflect the combined effects of finite-aperture size, variation of $|\vec{k}_1|$ with E , and the broadly peaked $\cos^2\omega_i$ factor that gives the directional selectivity of this technique.

It is interesting to note that the magnitude of the 3.7-Å peak in the $\vec{q} \parallel c$ RDF was about one-half the magnitude of the 1.4-Å peak in the $\vec{q} \perp c$ RDF, despite the fact that the average number of nearest neighbors at 3.6 Å is 3 times that at 1.4 Å. This is because the EXELFS oscillation for the $R = 3.6$ -Å peak are more strongly attenuated due to

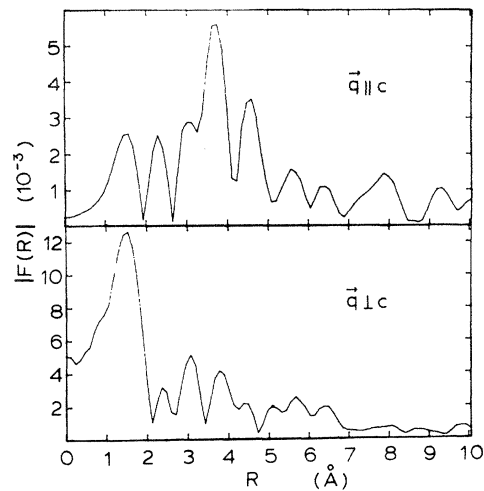


FIG. 3. Magnitudes of the Fourier transforms of the $k\chi(k)$ data shown in Fig. 2(b). Maxima in $|F(R)|$ occurred near 3.6 Å for $\vec{q} \parallel c$ and 1.4 Å for $\vec{q} \perp c$ as predicted.

the $e^{-2R_i/\lambda}$ and $e^{-2k^2\sigma_i^2}$ terms in Eq. (1). The second term gives a larger attenuation of the $R = 3.6$ -Å peak because σ_i^2 between the graphite planes is ~ 0.01 Å², while σ_i^2 for the nearest neighbors within the planes is 0.003 Å².²⁰

Similar to the EXAFS case, orientation-dependent EXELFS may become a powerful method for structural analysis. The main limitation is that in order to obtain directional sensitivity, only a small fraction of the inelastically scattered electrons can at present be accepted for analysis. In the future, however, more sophisticated detector designs should make possible a rapid analysis of several directions in a crystal simultaneously by collecting electrons scattered through different angles and energies all at the same time. We also note that electrons can usually be channeled through a crystal so that the electron-wave intensity peaks only at particular crystal sites.²¹ By a ready extension of the present method it should therefore be possible to analyze the near-neighbor environment of a particular type of atom located at a particular crystal site in a particular crystallographic direction.

Financial support from National Science Foundation Grant No. CHE791-6098, and Army Research Office Grant No. DAAG-29-80-0080 is gratefully acknowledged.

*Present address: Materials and Molecular Research Division, Lawrence Berkeley Laboratory, Berkeley, California 94720

- ¹S. M. Heald and E. A. Stern, *Phys. Rev. B* **16**, 5549 (1977).
- ²G. S. Brown, P. Eisenberger, and P. Schmidt, *Solid State Commun.* **24**, 201 (1977).
- ³P. Rabe, G. Tolkiehn, and A. Werner, *J. Phys. C* **13**, 1857 (1980).
- ⁴A. D. Cox and J. H. Beaumont, *Philos. Mag. B* **42**, 115 (1980).
- ⁵E. A. Stern, D. E. Sayers, J. G. Dash, H. Schecter, and B. Bunker, *Phys. Rev. Lett.* **38**, 767 (1977).
- ⁶S. M. Heald and E. A. Stern, *Phys. Rev. B* **17**, 4069 (1978).
- ⁷R. D. Leapman and V. E. Cosslet, *J. Phys. D* **9**, L29 (1976).
- ⁸B. M. Kincaid, A. E. Meixner, and P. M. Platzman, *Phys. Rev. Lett.* **36**, 326 (1978).
- ⁹P. E. Batson and A. J. Craven, *Phys. Rev. Lett.* **42**, 893 (1979).
- ¹⁰S. Csillag, D. E. Johnson, and E. A. Stern, in *EXAFS Spectroscopy*, edited by B. K. Teo and D. C. Joy (Plenum, New York, 1981), Chap. 19.
- ¹¹E. A. Stern, D. E. Sayers and F. W. Lytle, *Phys. Rev. B* **11**, 4836 (1975).
- ¹²R. D. Leapman, L. A. Grunes, P. L. Fejes, and J. Silcox, in *EXAFS Spectroscopy*, edited by B. K. Teo and D. C. Joy (Plenum, New York, 1981), Chap. 18.
- ¹³R. D. Leapman and J. Silcox, *Phys. Rev. Lett.* **42**, 1361 (1979).
- ¹⁴P. Goodman and G. Lehmpfuhl, *Acta Crystallogr.* **22**, 14 (1967).
- ¹⁵R. F. Egerton, *Philos. Mag.* **31**, (1975).
- ¹⁶P. A. Lee and G. Beni, *Phys. Rev. B* **15**, 2862 (1977).
- ¹⁷F. W. Lytle, D. E. Sayers, and E. A. Stern, *Phys. Rev. B* **11**, 4825 (1975).
- ¹⁸M. M. Disko, M. Sc. thesis, Arizona State University, 1980 (unpublished).
- ¹⁹B. K. Teo and P. A. Lee, *J. Am. Chem. Soc.* **101**, 2815 (1979).
- ²⁰R. Chen and P. Trucano, *Acta Crystallogr. A* **34**, 979 (1978).
- ²¹J. Taftø, *Z. Naturforsch.* **34a**, 452 (1979).